Three-Dimensional Structure of Solar Wind Turbulence

C. H. K. Chen,[1, *] A. Mallet,[2] A. A. Schekochihin,[2] T. S. Horbury,[3] R. T. Wicks,[3] and S. D. Bale[1, 4]

[1]*Space Sciences Laboratory, University of California, Berkeley, California 94720, USA*
[2]*Rudolf Peierls Centre for Theoretical Physics, University of Oxford, Oxford OX1 3NP, United Kingdom*
[3]*The Blackett Laboratory, Imperial College London, London SW7 2AZ, United Kingdom*
[4]*Physics Department, University of California, Berkeley, California 94720, USA*

We have measured, for the first time, the three-dimensional structure of inertial range plasma turbulence in the fast solar wind with respect to a local, physically motivated coordinate system. We found that the incompressible Alfvénic fluctuations are three-dimensionally anisotropic, with the sense of this anisotropy changing from large to small scales. At the largest scales, the magnetic field correlations are longest in the local fluctuation direction, consistent with Alfvén waves. At the smallest scales, they are longest along the local mean field direction and shortest in the direction perpendicular to the local mean field and the local field fluctuation. The compressive fluctuations are highly elongated along the local mean magnetic field direction, although axially symmetric perpendicular to it. Their large anisotropy may explain why they are not heavily damped.

Introduction.—The solar wind is a weakly collisional plasma [1] that is ubiquitously observed to be in a turbulent state [2–7]. Much progress has been made in understanding the nature of this turbulence since the first direct spacecraft observations [8, 9] but many aspects remain to be fully understood. In particular, the three-dimensional (3D) structure has been poorly characterized. Here, we use a new single-spacecraft technique to measure the 3D structure of turbulence in the fast solar wind.

Turbulence is usually modeled as a local cascade of fluctuations from large to small scales, forming an inertial range. In the solar wind, most of the inertial range energy is in Alfvénic fluctuations [10–12], which have magnetic field and velocity fluctuations perpendicular to the magnetic field direction [13]. Early isotropic magnetohydrodynamic (MHD) turbulence theories [14, 15] based on Kolmogorv scaling arguments [16] predict that the energy spectrum of weak Alfvénic turbulence is $E(k) \sim k^{-3/2}$, where k is the wavenumber of the fluctuations. Although 1D velocity power spectra in the solar wind at 1 AU display this scaling [17–19], the magnetic field has a $k^{-5/3}$ scaling [19–21].

It was later realized [22, 23] that the magnetic field direction can induce anisotropy in plasma turbulence. It was then proposed [24, 25] that Alfvénic turbulence tends towards a state of "critical balance," where the timescale of the Alfvénic fluctuations moving along the magnetic field is equal to the timescale of their nonlinear decay. This produces a spectrum perpendicular to the magnetic field of $E(k_\perp) \sim k_\perp^{-5/3}$, a parallel spectrum of $E(k_\parallel) \sim k_\parallel^{-2}$ and wavevector scaling $k_\parallel \sim k_\perp^{2/3}$. Solar wind measurements show evidence for both wavevector anisotropy of the form $k_\perp > k_\parallel$ [26–32] and a steeper spectral index parallel to the local magnetic field [28–33].

Critical balance theory was then extended to allow for the possibility that Alfvénic turbulence is 3D anisotropic [34]. The two special orthogonal directions are the mean magnetic field $\mathbf{B}_0$ and the perpendicular magnetic field fluctuation $\delta\mathbf{B}_\perp$. The theory assumes that the magnetic field and velocity
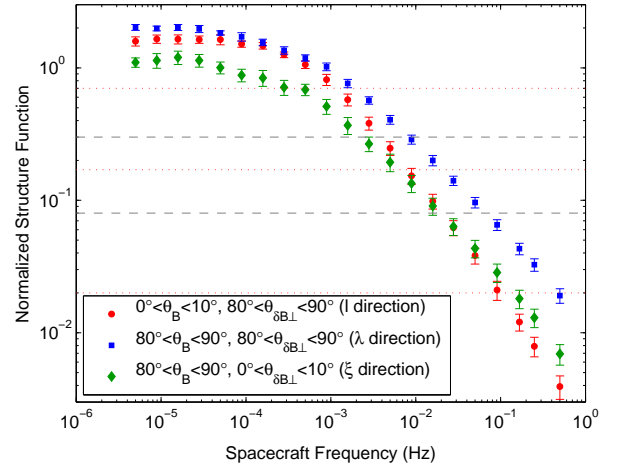

FIG. 1. Normalized **B**-trace structure function in three orthogonal directions. The grey dashed lines show the range of powers over which spectral indices were fitted.

fluctuations align to within a scale dependent angle θ_{ub}, which makes them 3D anisotropic: $l > \xi > \lambda$, where l, ξ and λ are their correlation lengths in the mean field direction $\mathbf{B}_0$, in the $\delta\mathbf{B}_\perp$ direction and perpendicular to both, respectively. The energy spectra implied by the theory in these three directions are $E(k_l) \sim k_l^{-2}$, $E(k_\xi) \sim k_\xi^{-5/3}$ and $E(k_\lambda) \sim k_\lambda^{-3/2}$.

Scale dependent alignment has been reported in the solar wind at large scales but it is difficult to measure this quantity deep in the inertial range due to instrumental limitations [35]. A recent multi-spacecraft measurement of the turbulent energy distribution in the near-Earth solar wind suggested that there was anisotropy with respect to global properties of the system, such as the global mean field, solar wind flow or the bow shock [36, 37]. As far as we are aware, there has not yet been a measurement of the 3D structure of solar wind turbulence in a local, scale-dependent coordinate system (l, ξ, λ).
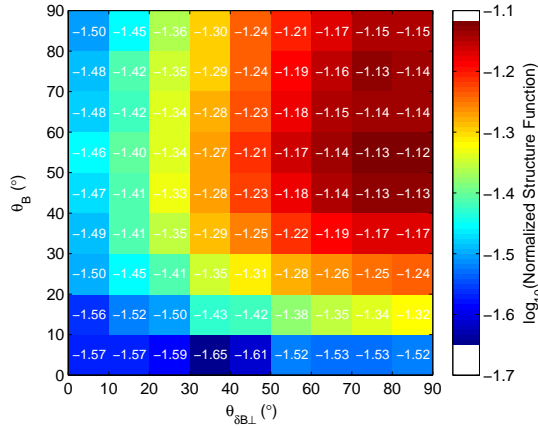
Although inertial range solar wind turbulence is predom-

FIG. 2. Normalized **B**-trace structure function at 1.5×10^{-2} Hz as a function of θ_B and $\theta_{\delta B_\perp}$.

FIG. 3. **B**-trace spectral index between normalized structure function values of 0.08 and 0.3 as a function of θ_B and $\theta_{\delta B_\perp}$.

inantly Alfvénic, there is also a non-negligible spectrum of slow mode [38] compressive fluctuations $\delta B_\parallel$ and δn, where n is the number density [19, 38–42]. The nature of these fluctuations is currently debated [43–45], in particular, the reason why they are not heavily damped [45]. Their structure has been less comprehensively characterized than the Alfvénic turbulence, although measurements in the magnetosheath show that there is some degree of 2D anisotropy [46, 47].

In this Letter, we present the first measurements of the scale-dependent 3D structure of Alfvénic and compressive magnetic field fluctuations ("eddies") with respect to a local coordinate system and discuss the implications for our understanding of plasma turbulence.

Method.—In the analysis, fast solar wind data from the Ulysses spacecraft [48] during a polar pass between 1.4 and 2.6 AU in days 100–299 of 1995 was used. The magnetic field data from VHM [49] was at 1 sec resolution and the velocity data from SWOOPS [50] was at 4 min resolution. The average solar wind speed was ≈ 780 km s^{-1} and the outer scale cross-helicity was moderately high, $\sigma_c \approx 0.6$ (other plasma parameters for this stream are given in [30]). The data was split into 10 intervals for the analysis.

For each 20 day interval, 21 logarithmically spaced spacecraft-frame frequencies at which to measure the power levels, over the range 5×10^{-6} Hz $\leq f_{sc} \leq 5 \times 10^{-1}$ Hz, were selected. For each of these frequencies, pairs of magnetic field measurements, $\mathbf{B}_1$ and $\mathbf{B}_2$, with the time lag $1/f_{sc}$ were chosen. For each pair, the contribution to the **B**-trace second order structure function $\sum_i (B_{1,i} - B_{2,i})^2$, where i is the component of the magnetic field, and the $|\mathbf{B}|$ second order structure function $(|\mathbf{B}_1| - |\mathbf{B}_2|)^2$ were calculated. Since most of the energy is in the perpendicular fluctuations [10, 11], the **B**-trace spectrum is a good proxy for the Alfvénic $\delta B_\perp$ spectrum and since $|\mathbf{B}| = |\mathbf{B}_0 + \delta\mathbf{B}| \approx \sqrt{|\mathbf{B}_0|^2 + 2\mathbf{B}_0 \cdot \delta\mathbf{B}} \approx |\mathbf{B}_0| + \delta B_\parallel$, the $|\mathbf{B}|$ spectrum is a good proxy for the compres-
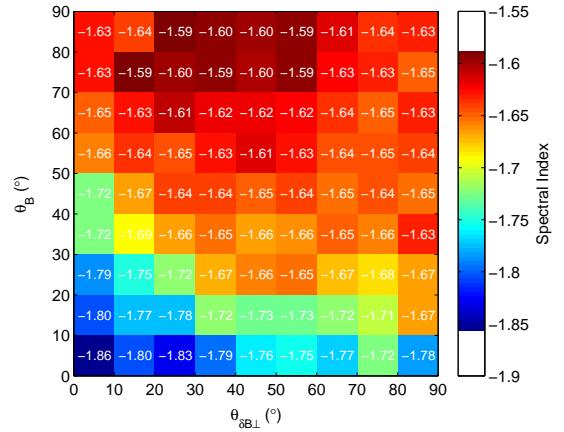
sive $\delta B_\parallel$ spectrum in the inertial range, where $|\delta\mathbf{B}| < |\mathbf{B}_0|$.

It has been shown [28, 31, 51, 52] that using a local scale-dependent coordinate system is essential for measuring 2D anisotropy. Here, this is extended by defining a local scale-dependent 3D coordinate system. For each pair of points, the local mean field $\mathbf{B}_{local} = (\mathbf{B}_1 + \mathbf{B}_2)/2$ and the local perpendicular fluctuation direction $\mathbf{B}_{local} \times [(\mathbf{B}_1 - \mathbf{B}_2) \times \mathbf{B}_{local}]$ were calculated. The angle between $\mathbf{B}_{local}$ and the solar wind velocity (which is the sampling direction), θ_B, and the angle between the local perpendicular fluctuation and the perpendicular component of the solar wind velocity, $\theta_{\delta B_\perp}$, were then found.

An orthogonal spherical polar coordinate system was defined, in which f_{sc} is the radial coordinate, θ_B is the polar angle and $\theta_{\delta B_\perp}$ is the azimuthal angle. It is in this local coordinate system that the 3D anisotropy of the turbulence was measured. The structure function contributions for each f_{sc} were binned with respect to θ_B and $\theta_{\delta B_\perp}$ and the mean value in each bin was calculated. Any angles greater than 90° were reflected to less than 90° to improve accuracy for scaling measurements. Reflection in $\theta_{\delta B_\perp}$ was found to be a good approximation; while there were few points to check the validity of reflection in θ_B, the assumption seems reasonable [29].

Taylor's hypothesis [53] can be assumed for this analysis: since the speed of the solar wind moving past the spacecraft is more than 10 times the Alfvén speed [30], temporal variations measured by the spacecraft, $1/f_{sc}$, correspond to spatial variations in the plasma v_{sw}/f_{sc}, where v_{sw} is the solar wind speed. This has been shown to be a good approximation [54].

Results: Alfvénic fluctuations.—Fig. 1 shows the **B**-trace structure function ("power") as a function of spaceraft-frame frequency for three angle bins corresponding to the $\mathbf{B}_{local}$ direction (red circles), the $\delta\mathbf{B}_\perp$ direction (green diamonds) and the direction perpendicular to both (blue squares). Each value is the mean calculated from the 10 intervals and the error bars are 2σ, where σ is the standard error of the mean. Before averaging, the structure functions of each interval were nor-
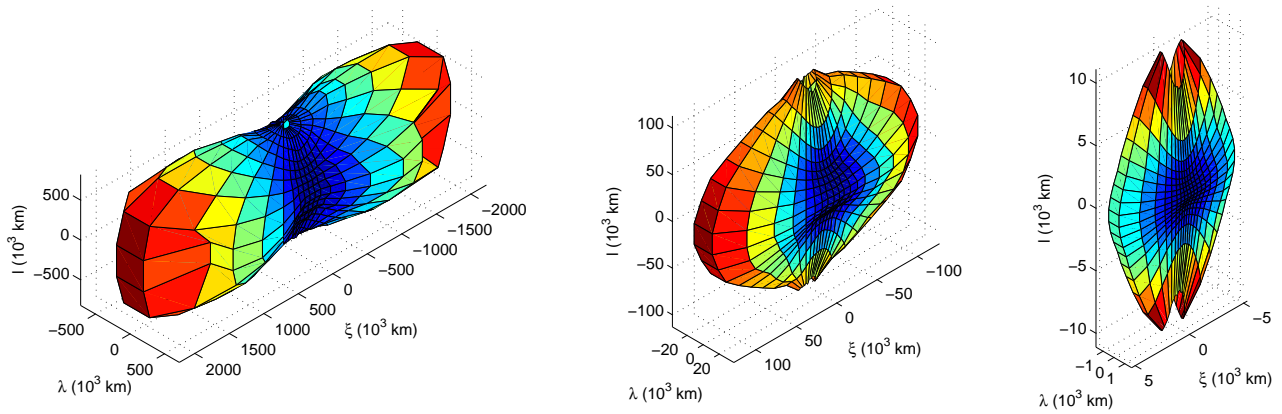
FIG. 4. Surfaces of constant **B**-trace power (statistical Alfvénic eddy shapes) from large (left) to small (right) scales. The normalized power levels are 0.7, 0.17 and 0.02 as marked with red dotted lines on Fig. 1. The typical proton gyroradius is ≈ 360 km.

malized to the square of the mean field strength over the interval $\langle|\mathbf{B}|\rangle^2$ to account for the varying power levels due to the spacecraft orbit. The typical proton gyroscale corresponds to a frequency ≈ 0.3 Hz.

The perpendicular (blue) curve is characteristic of fast solar wind: shallow in the low frequency $1/f_{\rm sc}$ range [55] and steeper in the higher frequency inertial range. The parallel (red) curve also matches previous parallel spectrum measurements, following the perpendicular curve at low frequencies, then becoming steeper than it in the inertial range [30]. The $\delta\mathbf{B}_\perp$ (green) curve has not previously been measured and describes how the 3D anisotropy evolves in the turbulent cascade. At large scales it has a smaller power than the other structure functions, which is consistent with this range consisting of Alfvén waves [10], since they have wavevectors in the plane perpendicular to $\delta\mathbf{B}_\perp$. It also remains at a lower power than the perpendicular structure function throughout the cascade but becomes larger than the parallel one at $\approx 3 \times 10^{-2}$ Hz.

For each 20 day interval, a power law was fitted to the normalized structure functions in each angle bin for powers between 0.08 and 0.3 (marked as grey dashed lines). A fixed power range, rather than a fixed $f_{\rm sc}$ range, was used so that the scaling was measured for the same set of fluctuations [56]. For each angle bin, the power law was evaluated at 1.5×10^{-2} Hz to give the 3D power anisotropy and the log of the mean of the 10 intervals is shown in Fig. 2. The typical standard error of the log of the mean is between 0.05 and 0.07. It can be seen that the power increases with both θ_B and $\theta_{\delta B_\perp}$, indicating 3D anisotropy, and seems to peak near $\theta_B = 60°$, $\theta_{\delta B_\perp} = 90°$.

Each fitted power law index was converted to a spectral index by subtracting 1 [57] and the 3D spectral index anisotropy is shown in Fig. 3. The typical standard error of the mean is 0.01 or 0.02, although the actual uncertainty may be larger due to systematic effects, such as the finite frequency response of the structure functions. The steepening towards small θ_B [28] can be seen but there appears to be little variation with $\theta_{\delta B_\perp}$

at large θ_B. The spectral index anisotropy was also calculated for normalized powers between 0.016 and 0.06, which is below the crossing point of the l and ξ spectra and close to the proton gyroscale. The spectra are steeper there, which may be because this is close to the dissipation range [58], with a scaling in the l direction of -1.87 ± 0.02, in the ξ direction of -1.72 ± 0.01 and in the λ direction of -1.74 ± 0.02.

To visualize how the 3D anisotropy varies through the turbulent cascade, surfaces of constant power were plotted. At a selected power level, the corresponding frequency in each angle bin was found through linear interpolation and the scale corresponding to these frequencies was calculated using Taylor's hypothesis. The scales, together with the angles θ_B and $\theta_{\delta B_\perp}$, were converted from spherical polar to Cartesian coordinates (l, ξ, λ) and the surfaces of constant power (at power levels marked by red dotted lines in Fig. 1) are shown in Fig. 4. They have been reflected into the other seven octants under the assumption of reflectional symmetry (see earlier). These statistical surfaces, in which color represents distance from the origin, can loosely be considered as average eddy shapes (although they are not eddies in the dynamical sense). It can be seen that they change from being extended in the $\delta\mathbf{B}_\perp$ direction in the large scale Alfvén wave range ($\xi > l, \lambda$) to being 3D anisotropic close to the proton gyroscale ($l > \xi > \lambda$). This anisotropy, however, does not appear to be a result of the 3D anisotropic scaling predicted by theory [34], but rather is due to Alfvén waves at large scales already possessing the $\xi > \lambda$ anisotropy and to the steeper scaling of the structure function in the mean field direction.

Results: compressive fluctuations.—The results of a similar analysis for the compressive fluctuations are shown in Fig. 5 (where the structure functions have been normalized in the same way as for the Alfvénic fluctuations in Fig. 1) and Fig. 6, which is the surface of constant normalized power of 1.2×10^{-3} (marked as a red dotted line in Fig. 5). It can be seen that their structure is different to the Alfvénic fluctuations: there is no anisotropy in the plane perpendicular to the mean field,
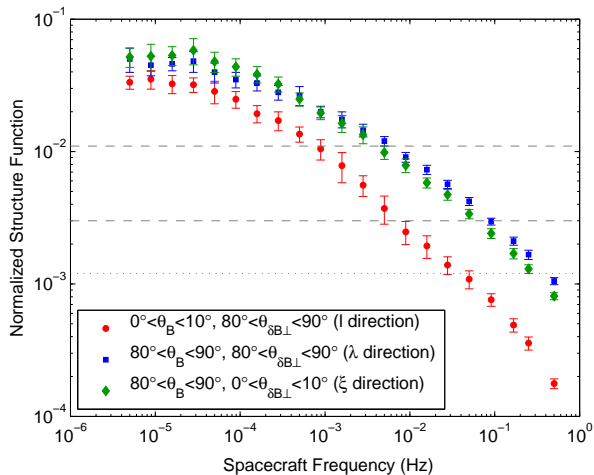
FIG. 5. Normalized $|\mathbf{B}|$ structure function in three orthogonal directions. The grey dashed lines show the range of powers over which spectral indices were fitted.

FIG. 6. Surface of constant $|\mathbf{B}|$ power (statistical compressive eddy shape) at small scales. The normalized power level is 1.2×10^{-3} as marked with a red dotted line on Fig. 5.

which means that the compressive fluctuations do not depend on the polarization of the Alfvénic fluctuations. Also, they are more elongated along the mean field direction than the Alfvénic fluctuations: for a given perpendicular scale λ the ratio l/λ is at least 2 or 3 times larger. Due to limited angular resolution this is a lower limit; by extrapolating the shape in Fig. 6 one could imagine that they are even more extended than can currently be measured.

The spectral indices of $|\mathbf{B}|$ for normalized powers between 3×10^{-3} and 1.1×10^{-2} are between –1.42 and –1.58 in all angle bins, with a typical standard error of the mean of 0.02. This is different to the slow solar wind, where spectral indicies close to –5/3 are observed [19]. This difference has also been noticed in the electron density spectrum [42], although the reason is not well understood. If the compressive fluctuations are indeed very anisotropic, then we would not expect to measure the true parallel spectral index with the current angular resolution, which may explain the presence of anisotropic structures yet no significant anisotropic scaling.

Discussion.—Although we have shown that the Alfvénic fluctuations are 3D anisotropic in shape, no evidence of 3D anisotropic scaling was found: structure functions with respect to ξ and λ scale the same. Since the alignment angle between the magnetic field and velocity fluctuations is expected to scale as $\theta_{ub} \sim \lambda/\xi$ [34], this suggests that θ_{ub} is constant and there is no scale dependent alignment. It is possible that this is because in the fast solar wind at a few AU, the turbulence is driven in a highly anisotropic way: the large-scale Alfvén waves have $\xi > l, \lambda$. This situation persists deep into the inertial range: $\xi > l$, rather than $\xi/l \sim |\delta\mathbf{B}|/|\mathbf{B}| < 1$, as would be required for critical balance and for the theory [34] to apply. The theoretically envisioned regime $l > \xi > \lambda$ is only reached at $f_{\rm sc} \approx 10^{-1}$ Hz, close to the proton gyroscale, which is where the inertial range ends. It is possible that with a longer inertial range, the 3D anisotropic scaling may develop
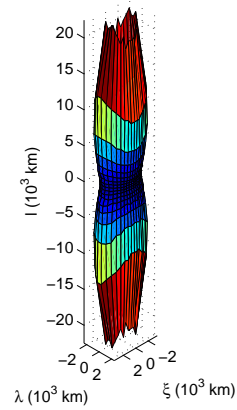
once $l \gg \xi, \lambda$ is well satisfied, which may be the case in other areas of the solar wind (e.g., farther away from the Sun and/or in the slow wind). Indeed, using the same method as described here to measure turbulence in reduced MHD simulations with $|\delta\mathbf{B}|/|\mathbf{B}| \ll 1$ and driven (approximately) in critical balance, different scalings in all three directions were found and the situation $l > \xi > \lambda$ was seen to develop at small scales [59].

The fact that the compressive fluctuations were measured to be very elongated is consistent with the prediction, based on gyrokinetic theory, that they are passive to the Alfvénic fluctuations, but have no parallel cascade along the exact magnetic field lines [45]. This may explain why there is a compressive cascade in the solar wind: the compressive fluctuations are expected to be damped at a rate proportional to their parallel wavenumber $\gamma \sim k_\parallel$ [45] but if $k_\parallel$ is very small then they are not heavily damped and can cascade nonlinearly.

Figs. 2, 3, 4 and 6 also reveal the structure of the turbulence at intermediate angles that are not directly in the l, ξ or λ directions. There are currently no theoretical predictions for the full 3D eddy shapes and this structure remains to be explained. Other obvious extensions of this work include measuring the 3D structure in slow solar wind [31], of other fields such as velocity and the Elsasser variables [32], and in the small scale cascade below the ion gyroscale [58].

* chen@ssl.berkeley.edu
[1] J. C. Kasper, A. J. Lazarus, and S. P. Gary, Phys. Rev. Lett. **101**, 261103 (2008).
[2] C.-Y. Tu and E. Marsch, Space Sci. Rev. **73**, 1 (1995).
[3] M. L. Goldstein, D. A. Roberts, and W. H. Matthaeus,

Ann. Rev. Astron. Astrophys. **33**, 283 (1995).

[4] T. S. Horbury, M. A. Forman, and S. Oughton, Plasma Phys. Control. Fusion **47**, B703 (2005).

[5] R. Bruno and V. Carbone, Living Rev. Solar Phys. **2**, 4 (2005).

[6] A. Petrosyan, A. Balogh, M. L. Goldstein, J. Léorat, E. Marsch, K. Petrovay, B. Roberts, R. von Steiger, and J. C. Vial, Space Sci. Rev. **156**, 135 (2010).

[7] W. H. Matthaeus and M. Velli, Space Sci. Rev. (2011), doi:10.1007/s11214-011-9793-9.

[8] G. L. Siscoe, L. Davis, Jr., P. J. Coleman, Jr., E. J. Smith, and D. E. Jones, J. Geophys. Res. **73**, 61 (1968).

[9] P. J. Coleman, Astrophys. J. **153**, 371 (1968).

[10] J. W. Belcher and L. Davis, J. Geophys. Res. **76**, 3534 (1971).

[11] T. S. Horbury, A. Balogh, R. J. Forsyth, and E. J. Smith, Geophys. Res. Lett. **22**, 3405 (1995).

[12] S. D. Bale, P. J. Kellogg, F. S. Mozer, T. S. Horbury, and H. Reme, Phys. Rev. Lett. **94**, 215002 (2005).

[13] H. Alfvén, Nature (London) **150**, 405 (1942).

[14] P. S. Iroshnikov, Astron. Zh. **40**, 742 (1963) [Sov. Astron. **7**, 566 (1964)].

[15] R. H. Kraichnan, Phys. Fluids **8**, 1385 (1965).

[16] A. Kolmogorov, Dok. Akad. Nauk SSSR **30**, 301 (1941).

[17] J. J. Podesta, D. A. Roberts, and M. L. Goldstein, Astrophys. J. **664**, 543 (2007).

[18] C. Salem, A. Mangeney, S. D. Bale, and P. Veltri, Astrophys. J. **702**, 537 (2009).

[19] C. H. K. Chen, S. D. Bale, C. Salem, and F. S. Mozer, Astrophys. J. **737**, L41 (2011).

[20] W. H. Matthaeus and M. L. Goldstein, J. Geophys. Res. **87**, 6011 (1982).

[21] C. W. Smith, K. Hamilton, B. J. Vasquez, and R. J. Leamon, Astrophys. J. **645**, L85 (2006).

[22] D. Montgomery and L. Turner, Phys. Fluids **24**, 825 (1981).

[23] J. V. Shebalin, W. H. Matthaeus, and D. Montgomery, J. Plasma Phys. **29**, 525 (1983).

[24] J. C. Higdon, Astrophys. J. **285**, 109 (1984).

[25] P. Goldreich and S. Sridhar, Astrophys. J. **438**, 763 (1995).

[26] N. U. Crooker, G. L. Siscoe, C. T. Russell, and E. J. Smith, J. Geophys. Res. **87**, 2224 (1982).

[27] J. W. Bieber, W. Wanner, and W. H. Matthaeus, J. Geophys. Res. **101**, 2511 (1996).

[28] T. S. Horbury, M. Forman, and S. Oughton, Phys. Rev. Lett. **101**, 175005 (2008).

[29] J. J. Podesta, Astrophys. J. **698**, 986 (2009).

[30] R. T. Wicks, T. S. Horbury, C. H. K. Chen, and A. A. Schekochihin, Mon. Not. R. Astron. Soc. **407**, L31 (2010).

[31] C. H. K. Chen, A. Mallet, T. A. Yousef, A. A. Schekochihin, and T. S. Horbury, Mon. Not. R. Astron. Soc. **415**, 3219 (2011).

[32] R. T. Wicks, T. S. Horbury, C. H. K. Chen, and A. A. Schekochihin, Phys. Rev. Lett. **106**, 045001 (2011).

[33] Q. Y. Luo and D. J. Wu, Astrophys. J. **714**, L138 (2010).

[34] S. Boldyrev, Phys. Rev. Lett. **96**, 115002 (2006).

[35] J. J. Podesta, B. D. G. Chandran, A. Bhattacharjee, D. A. Roberts, and M. L. Goldstein, J. Geophys. Res. **114**, 1107 (2009).

[36] Y. Narita, K.-H. Glassmeier, F. Sahraoui, and M. L. Goldstein, Phys. Rev. Lett. **104**, 171101 (2010).

[37] Y. Narita, F. Sahraoui, M. L. Goldstein, and K.-H. Glassmeier, J. Geophys. Res. **115**, 4101 (2010).

[38] G. G. Howes, S. D. Bale, K. G. Klein, C. H. K. Chen, C. S. Salem, and J. M. TenBarge, arXiv:1106.4327v1 (2011).

[39] E. Marsch and C.-Y. Tu, J. Geophys. Res. **95**, 11945 (1990).

[40] C. Tu and E. Marsch, J. Geophys. Res. **99**, 21481 (1994).

[41] B. Hnat, S. C. Chapman, and G. Rowlands, Phys. Rev. Lett. **94**, 204502 (2005).

[42] K. Issautier, A. Mangeney, and O. Alexandrova, AIP Conf. Proc. **1216**, 148 (2010).

[43] W. H. Matthaeus, L. W. Klein, S. Ghosh, and M. R. Brown, J. Geophys. Res. **96**, 5421 (1991).

[44] Y. Lithwick and P. Goldreich, Astrophys. J. **562**, 279 (2001).

[45] A. A. Schekochihin, S. C. Cowley, W. Dorland, G. W. Hammett, G. G. Howes, E. Quataert, and T. Tatsuno, Astrophys. J. Suppl. **182**, 310 (2009).

[46] O. Alexandrova, C. Lacombe, and A. Mangeney, Ann. Geophys. **26**, 3585 (2008).

[47] J.-S. He, E. Marsch, C.-Y. Tu, Q.-G. Zong, S. Yao, and H. Tian, J. Geophys. Res. **116**, A06207 (2011).

[48] K. P. Wenzel, R. G. Marsden, D. E. Page, and E. J. Smith, Astron. Astrophys. Suppl. Ser. **92**, 207 (1992).

[49] A. Balogh, T. J. Beek, R. J. Forsyth, P. C. Hedgecock, R. J. Marquedant, E. J. Smith, D. J. Southwood, and B. T. Tsurutani, Astron. Astrophys. Suppl. Ser. **92**, 221 (1992).

[50] S. J. Bame, D. J. McComas, B. L. Barraclough, J. L. Phillips, K. J. Sofaly, J. C. Chavez, B. E. Goldstein, and R. K. Sakurai, Astron. Astrophys. Suppl. Ser. **92**, 237 (1992).

[51] J. Cho and E. T. Vishniac, Astrophys. J. **539**, 273 (2000).

[52] J. Maron and P. Goldreich, Astrophys. J. **554**, 1175 (2001).

[53] G. I. Taylor, Proc. R. Soc. London A **164**, 476 (1938).

[54] Y. Narita, K.-H. Glassmeier, and U. Motschmann, Nonlin. Processes Geophys. **17**, 383 (2010).

[55] W. H. Matthaeus and M. L. Goldstein, Phys. Rev. Lett. **57**, 495 (1986).

[56] C. H. K. Chen, R. T. Wicks, T. S. Horbury, and A. A. Schekochihin, Astrophys. J. **711**, L79 (2010).

[57] A. S. Monin and A. M. Yaglom, *Statistical Fluid Mechanics, Vol 2* (MIT Press, 1975).

[58] C. H. K. Chen, T. S. Horbury, A. A. Schekochihin, R. T. Wicks, O. Alexandrova, and J. Mitchell, Phys. Rev. Lett. **104**, 255002 (2010).

[59] A. Mallet, A. A. Schekochihin, C. H. K. Chen, T. S. Horbury, R. T. Wicks, and T. A. Yousef, Phys. Rev. Lett. (in preparation) (2011).